

Cite this: *Dalton Trans.*, 2018, 47, 4428Received 10th January 2018,
Accepted 6th February 2018

DOI: 10.1039/c8dt00110c

rsc.li/dalton

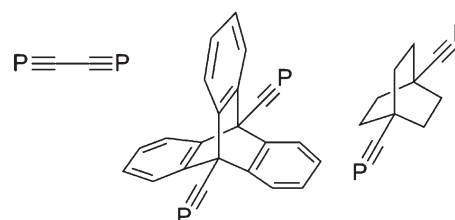
Through-conjugation of two phosphalkyne ('C≡P') moieties mediated by a bimetallic scaffold †

Matthew. C. Leech and Ian R. Crossley *

Through-conjugation of two phosphalkyne moieties within an isolable molecule is demonstrated for the first time with the synthesis of $[\{\text{Ru}(\text{dppe})_2\}_2\{\mu\text{-(C}\equiv\text{C)}_2\text{C}_6\text{H}_4\text{-}p\}\{\text{C}\equiv\text{P}\}_2]$, via base-induced desilylation of $[\{\text{Ru}(\text{dppe})_2\}_2\{\mu\text{-(C}\equiv\text{C)}_2\text{C}_6\text{H}_4\text{-}p\}\{\eta^1\text{-P}\equiv\text{CSiMe}_3\}_2]^{2+}$. The nature of the cyaphide ligands and their influence upon the bimetallic core are studied electrochemically.

Phosphaalkynes ($\text{RC}\equiv\text{P}$)¹ are archetypal models of the phosphorus–carbon analogy,² being both isolobal and isoelectronic with alkynes. Though dichotomous in nature – by virtue of the polarity and lone-pair imparted by phosphorus – their chemical analogy to alkynes is well-established, with a prevalence of cycloaddition/oligomerisation reactions, while both $\eta^2\text{-CP}$ (*cf.* alkynes) and $\eta^1\text{-P}$ (*cf.* nitriles, alkynyls) complexes with transition metals are known.³ Notwithstanding, an enduring omission lies with the incorporation of the discrete 'C≡P' moiety into architectures featuring extended conjugation (*cf.* the prevalence of polyacetylenes), a desirable target – particularly from an organometallic standpoint⁴ – given extensive interest in acetylenic and phosphorus-containing moieties in the context of developing molecular electronic components.^{5–7} Indeed, the conjugation of phosphalkyne ('C≡P') moieties with other π -systems is limited to the small range of aromatic phosphaalkynes: $\text{PhC}\equiv\text{P}$,⁸ 2,6- $\text{R-C}_6\text{H}_3\text{C}\equiv\text{P}$ ($\text{R} = \text{Mes}, \text{tBu}$),⁹ 2,6- $\text{R-4-R}'\text{-C}_6\text{H}_2\text{C}\equiv\text{P}$ ($\text{R} = \text{tBu}, \text{R}' = \text{OMe}, \text{NMe}_2$,^{9b} $\text{R}=\text{R}' = \text{tBu}$,¹⁰ $\text{CMe}_2\text{Et}^{11}$) and the putative $\text{P}\equiv\text{C-C}\equiv\text{E}$ ($\text{E} = \text{CH}, \text{N}$,^{12a,b} P^{12c-e}), which were generated (transiently) and observed in the gas phase. The latter ($\text{P}\equiv\text{C-C}\equiv\text{P}$) is also among a very limited range of compounds to feature two 'C≡P' moieties (Chart 1),¹³ and is the sole precedent example for which their mutual conjugation might reasonably be invoked (albeit unstudied).

Though a small number of transition metal complexes featuring *trans*-disposed η^1 -phosphaalkynes has been reported,¹⁴

Chart 1 Known bis-phosphaalkynes.^{12,13}

viz. $[\text{M}(\text{L})_2(\text{P}\equiv\text{C}^t\text{Bu})_2]$ ($\text{M} = \text{Mo}, \text{L} = \text{dppe}, \text{depe}, \text{R}_2\text{PC}_2\text{H}_4\text{PR}_2$, $\text{R} = \text{Tol}, \text{ClC}_6\text{H}_4$); ($\text{M} = \text{W}, \text{L} = \text{dppe}$), $[\text{Mo}(\text{depe})_2(\text{P}\equiv\text{CAD})_2]$ and $[\text{Mo}(\text{dppe})_2(\text{P}\equiv\text{CSiMe}_3)_2]$,¹⁵ even the concept of metal-mediated conjugation (*cf.* bis-alkynyl complexes) was unexplored prior to our recent report of the unprecedented cyaphide–alkynyl complexes *trans*- $[\text{Ru}(\text{dppe})_2(\text{C}\equiv\text{CR})(\text{C}\equiv\text{P})]$ ($\text{R} = \text{CO}_2\text{Me}, p\text{-An}$).¹⁶ Herein, we extend this conceptual framework to consider, for the first time, extended conjugation between multiple 'C≡P' moieties, mediated by a bimetallic, redox-active, core; we also elucidate the electronic and redox nature of these complexes.

The sequential treatment of the bisethynylbenzene-bridged bimetallic complex $[\{\text{Ru}(\text{dppe})_2\}_2\{\mu\text{-(C}\equiv\text{C)}_2\text{C}_6\text{H}_4\text{-}p\}\text{Cl}_2]$ (**1**) with two equivalents of AgOTf and $\text{P}\equiv\text{CSiMe}_3$ facilitates installation of two terminal phosphalkyne moieties to afford **2**²⁺ (Scheme 1). Formation of **2**²⁺ is evident from characteristic spectroscopic signatures indicative of a coordinated phosphalkyne ($\delta_{\text{P}} 111.4$, $J_{\text{PP}} 34$ Hz) in proximity to the dppe scaffold ($\delta_{\text{P}} 42.2$ (1:4 ratio)), while the carbon-rich bridge remains apparent from $^{13}\text{C}\{\text{H}\}$ NMR and infrared ($\nu_{\text{C}\equiv\text{C}} 2054 \text{ cm}^{-1}$) spectroscopic data. Retention of the silyl moieties follows from heteronuclear ($^1\text{H}\text{-}^{29}\text{Si}$) correlation, while the triflate counter-ion is observed in the ^{19}F -NMR spectrum ($\delta_{\text{F}} -78.9$); bulk composition is affirmed by microanalysis.

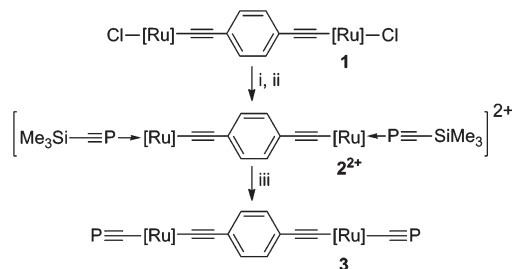
The connectivity of **2**²⁺ is further supported by X-ray diffraction data (Fig. 1).¹⁷ The internal geometry is largely unremarkable, exhibiting only slight deviations from linearity about the metal centres ($\angle \text{P-Ru-C } 173.4(2), 175.3(2)^\circ$) and in the bridge

Department of Chemistry, University of Sussex, Brighton, UK.

E-mail: i.crossley@sussex.ac.uk; Fax: +44 (0)1273876678; Tel: +44 (0)1273 877302

† Electronic supplementary information (ESI) available: Synthetic procedures, characterising data and spectra, computational and electrochemical details, orbital plots, X-ray diffraction data. CCDC 1811689. For ESI and crystallographic data in CIF or other electronic format see DOI: 10.1039/c8dt00110c





Scheme 1 Reagents and conditions: (i) CH_2Cl_2 , 2 AgOTf, (ii) 2 $\text{P}\equiv\text{CSiMe}_3$ in toluene, 1 h.; (iii) thf, 2 KO^tBu , 1 h. [Ru] = $\text{Ru}(\text{dppe})_2$.

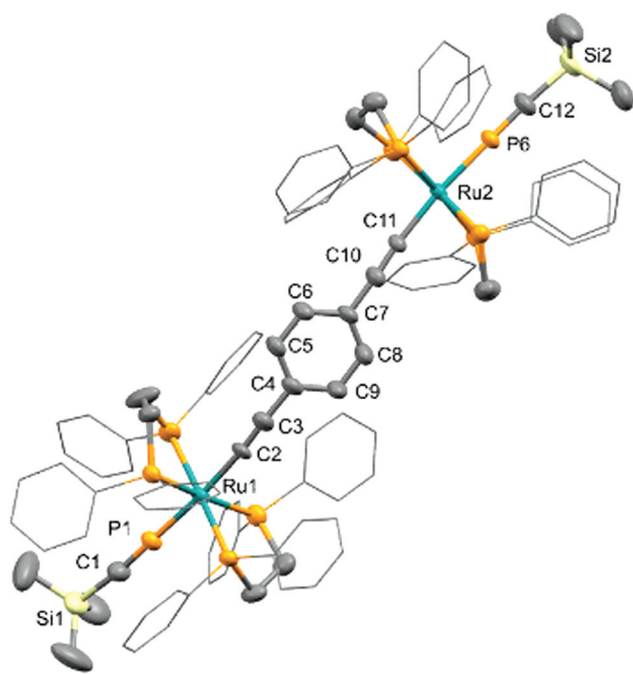


Fig. 1 Molecular structure of 2^{2+} ; 50% thermal ellipsoids, hydrogen atoms omitted, and phenyl rings reduced for clarity. Selected bond distances (Å) and angles ($^\circ$): Ru1–P1 2.264(1), Ru1–C2 2.035(4), Ru2–P6 2.269(1), Ru1–C11 2.022(4), P1–C1 1.526(5), C2–C3 1.203(6), C3–C4 1.443(6), P6–C12 1.526(5), C10–C11 1.214(6), C10–C7 1.441(6); P1–Ru1–C2 175.23(13), P6–Ru2–C11 173.38(12), C1–P1–Ru1 179.3(2), C12–P6–Ru2 177.3(2), Ru1–C2–C3 174.2(4), Ru2–C11–C10 174.5(4), C2–C3–C4 171.7(5), C11–C10–C7 174.8(5).

(\angle Ru–C \equiv C 174.5(4), 174.2(4); \angle C \equiv C–C 174.5(5), 172.7(5) $^\circ$) characteristic, respectively, of other bis-alkynyls¹⁸ and the limited range of structurally characterized complexes comprising the ' $\text{Ru}_2\{\mu\text{-(C}\equiv\text{C)}_2\text{C}_6\text{H}_4\text{-}p\}$ ' and related cores.¹⁹ The coordinated phosphalkyne moieties are similarly consistent with related analogues.^{14–16,20}

Conversion of the $\eta^1\text{-P}\equiv\text{CSiMe}_3$ moieties to terminal cyaphide ligands ($\text{-C}\equiv\text{P}$) proceeds upon treating 2^{2+} with 2 equiv. KO^tBu ,²¹ affording **3** in moderate yield (Scheme 1). While single crystals of **3** can be grown, their rapid desolvation during mounting (even at low temperature) has precluded the

Table 1 Comparative experimental and calculated NMR spectroscopic data^a

	$\delta_{\text{P}(\text{CP})}$	$\Delta\delta_{\text{P}(\text{CP})}^b$	$\delta_{\text{C}(\text{CP})}$	$\Delta\delta_{\text{C}(\text{CP})}^b$
2^{2+}	111.4	—	189.8	—
3	159.7	48.3	281.8	92.0
$[\{\text{Ru}\}(\text{C}_2\text{R})(\text{P}\equiv\text{CSiMe}_3)]^+$	108.4	—	192.6	—
$[\{\text{Ru}\}(\text{C}_2\text{R})(\text{C}\equiv\text{P})]$ (R = CO_2Me)	168.5	60.0	279.1	86.5
$[\{\text{Ru}\}(\text{C}_2\text{R})(\text{P}\equiv\text{CSiMe}_3)]^+$	112.8	—	188.2	—
$[\{\text{Ru}\}(\text{C}_2\text{R})(\text{C}\equiv\text{P})]$ (R = <i>p</i> -An)	159.5	46.7	281.9	93.7
$[\{\text{Ru}\}\text{H}(\text{P}\equiv\text{CSiPh}_3)]^{+20a}$	143.8 ^c	—	175.1	—
$[\{\text{Ru}\}\text{H}(\text{C}\equiv\text{P})]^{20a}$	165.0	21.3	287.1	112.0
2^{2+} (calc) ^d	118.4	—	188.8	—
3 (calc) ^d	166.4	48.0	271.4	82.6

^a [Ru] = $\text{Ru}(\text{dppe})_2$. ^b $\Delta\delta$ on conversion from $\eta^1\text{-P}\equiv\text{CR}$ to terminal cyaphide. ^c Increase in δ_{P} due to SiPh_3 vs. SiMe_3 . ^d GIAO method with the PBE functional (lanl2dz for Ru; 6-31G** for all other atoms); referenced to H_3PO_4 or Me_4Si at the same level of theory.

acquisition of X-ray diffraction data. Nonetheless, the identity of **3** is readily established from the characteristic spectroscopic features and changes that accompany the desilylative rearrangement of $\eta^1\text{-P}\equiv\text{CSiMe}_3$ to cyaphide;^{16,20a} viz. (i) reduction in frequency of the C \equiv P stretch ($\Delta\nu_{\text{C}\equiv\text{P}} \sim -12 \text{ cm}^{-1}$); (ii) loss of NMR resonances for silyl and OTf moieties; (iii) increase in frequency ($\Delta\delta_{\text{P}}$ 48) for the phosphalkynic P-centres, with reduced magnitude of the $\text{P}_{\text{CP}}\text{-P}_{\text{dppe}}$ coupling (precluding its resolution); (iv) increased frequency ($\Delta\delta_{\text{C}}$ 92) for the cyaphidic carbon resonance, consistent with formation of an organometallic linkage (*cf* M–CO, M–CN). These data compare well with those we have noted previously¹⁶ and those for Grutzmacher's seminal complex $[\text{RuH}(\text{dppe})_2(\text{C}\equiv\text{P})]$;^{20a} they also concur with data calculated for **3** using the PBE functional (Table 1).

The optimized gas-phase geometries of 2^{2+} and **3** (see ESI[†])²² both exhibit slightly greater linearity about the metal centres and bridge when compared with the solid-state structure of 2^{2+} , alongside marginally longer C \equiv P linkages ($\sim 1.58 \text{ \AA}$). These features are consistent with a prevalence of packing effects in the solid state, as noted previously for several $\eta^1\text{-P}\equiv\text{CR}$ complexes,^{20,23} and for our precedent cyaphide-alkynyls.¹⁶ The calculated C \equiv P stretching mode for **3** (asym. $\nu_{\text{C}\equiv\text{P}}$ 1224 cm^{-1}) also compares well with experiment ($\nu_{\text{C}\equiv\text{P}}$ 1247 cm^{-1}). Notably, the experimentally observed frequency reflects a slightly stronger C \equiv P linkage for **3** than in $[\text{RuH}(\text{dppe})_2(\text{C}\equiv\text{P})]$ ($\nu_{\text{C}\equiv\text{P}}$ 1239 cm^{-1}),^{20a} attributable to competition with the *trans*-alkynyl for $\text{Ru} \rightarrow \pi^*$ donation. Indeed, we noted this previously for cyaphide-alkynyls, though to a greater extent ($\nu_{\text{C}\equiv\text{P}}$ 1255, 1260 cm^{-1}),¹⁶ suggesting a reduced competition within the bimetallic scaffold.

The frontier orbitals of 2^{2+} and **3** (Fig. 2) show similarities, the HOMO in each case being dominated by the bridging π -system (76%, 2^{2+} ; 54% **3**) with a modest contribution from the metals (14% 2^{2+} ; 26% **3**). Notably, the HOMO of **3** also includes contributions from $\pi_{\text{C}\equiv\text{P}}$ (14%), which engage in out-of-phase mixing with the Ru (d_{xy} , d_{xz}), $\pi_{\text{C}\equiv\text{C}}$ and π_{Ar} orbitals, consistent with some level of through-conjugation. The contri-



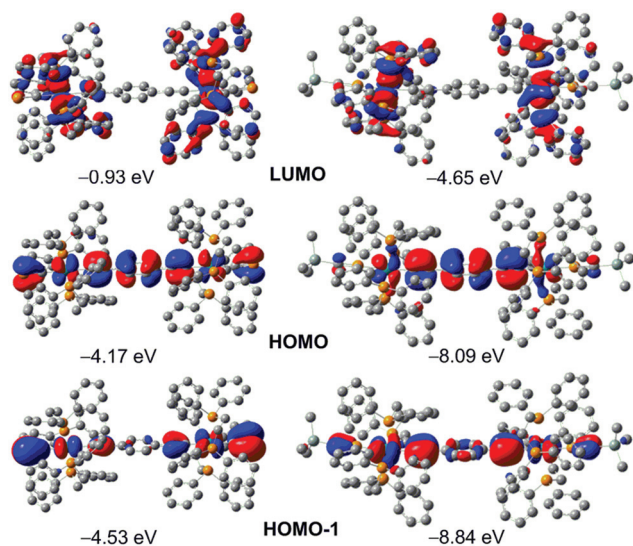


Fig. 2 Frontier orbitals for **3** (left) and 2^{2+} (right), with relative energies (see also ESI†).

Contributions from $\pi_{C\equiv P}$ increase appreciably in the mutually degenerate HOMO–1 and HOMO–2 (~25%, see ESI†), lying 0.36 eV below the HOMO, albeit without involvement of the bridging arene (1%). In marked contrast, there is negligible contribution (<10%) from the $\eta^1\text{-P}=\text{CSiMe}_3$ moieties of 2^{2+} to any occupied frontier orbitals, their involvement becoming significant only in the appreciably stabilized HOMO–3 and HOMO–4, lying *ca.* 1.4 eV below the HOMO. Finally, in respect of **3**, we note that the terminal cyaphidic lone-pairs manifest in the HOMO–14 and HOMO–15, being stabilised by *ca.* 2 eV relative to the HOMO. This is entirely consistent with expectation, being similar to our previous observations,¹⁶ and those for phosphalkynes more generally.²⁴ Additionally, NBO calculations suggest these to reside in orbitals of *ca.* 75% *s* and 25% *p* character, as is typical of phosphalkynes.

As is typical of complexes with the Ru(dppe)₂ scaffold, the latter dominates the virtual orbitals of **3**, which are mostly centred on the dppe ligands; the bridge contributes marginally to LUMO+12 and LUMO+14, lying 4 eV above the HOMO. In contrast, while the LUMO/LUMO+1 of 2^{2+} are again dominated by the Ru(dppe)₂ framework, LUMO+2 is centred on the unsaturated core, with appreciable contributions from $\pi^*_{C\equiv P}$ (60%) and the bridge (15%). This is reflected in the electronic spectrum of 2^{2+} , assigned in comparison with those derived from TD-DFT studies,²⁵ calculating the first 200 excited states. This offers a fair approximation of the observed UV spectra for 2^{2+} and **3** (within limitations of the model), providing sufficient correlation to assist in the assignment of some key features. Thus, a feature at 350 nm (28 571 cm⁻¹) includes significant contribution from LLCT bands ($\pi_{C=C} \rightarrow \pi^*_{Ar}$ and $\pi_{C=C} \rightarrow \pi^*_{C\equiv P}$) with marginal involvement of intraligand CT ($\pi_{C=C} \rightarrow \pi^*_{C=C}$), alongside the dominant MLCT and LLCT associated with excitation from the HOMO/HOMO+1 to low-lying dppe-based orbitals. A second feature around 260 nm (38 462 cm⁻¹) is

Table 2 Electrochemical (CV) data and comproportionation constants^{a,b}

	E_{pa}/V	E_{pc}/V	$E_{1/2}(\Delta E_{pp})/V$	$\Delta E_{pa}/V$	K_c^b
1	-0.268	-0.348	-0.308 (80)	0.351	8.9×10^5
	0.081	0.004	0.043 (77)		
2^{2+}	0.705	0.565	0.635 (140)	0.290	0.8×10^5
	0.995				
3	-0.210 ^c	-0.780 ^d	—	0.190	1.7×10^3
	-0.020 ^c				

^a CH₂Cl₂/0.1 M [NBu₄]PF₆ using 1 mM analyte solutions at (25 °C), with Pt disc (1 mm) working electrode, Pt wire counter electrode and Ag wire pseudo-reference at 100 mV s⁻¹. Potentials relative to the FcH/FcH⁺ couple (0.00 V), referenced using internal Fc*H/Fc*H⁺ (-0.56 V (E_{pp} 78 mV) vs. Fc/Fc⁺). ^b $K_c = 10^{\Delta E/59 \text{ mV}}$ at 298 K. ^c Irreversible oxidation. ^d Irreversible reduction.

primarily composed of ILCT within the dppe scaffold (<HOMO–10 → LUMO), but with additional contribution from $\pi_{C\equiv P} \rightarrow \pi^*_{C\equiv P}$ ILCT and $\pi_{Ar} \rightarrow \pi^*_{C\equiv P}$ LLCT (HOMO–3 → LUMO+5). In contrast, features in the UV/Vis spectrum of **3** around 370 nm (27 027 cm⁻¹) and 250 nm (40 000 cm⁻¹) are wholly dominated by MLCT and LLCT transitions to the dppe scaffold, with marginal contributions from ILCT within the bridging π -framework; contributions from transitions to the high-lying $\pi^*_{C\equiv P}$ (LUMO+36 to LUMO+39) are negligible.

The redox behaviours of 2^{2+} and **3** were explored using cyclic voltammetry (Table 2 and ESI†), both compounds exhibiting two distinct oxidative events, which can be assigned (trivially²⁶) to sequential generation of the Ru^{III}/Ru^{II} and Ru^{III}/Ru^{III} species. For 2^{2+} an initial quasi-reversible oxidation occurs at significantly more anodic potential than the corresponding (reversible) feature of **1**, presumably a corollary of its cationic nature. The second (irreversible) oxidation is similarly shifted to more positive potential,²⁷ and demonstrates an appreciable stability for the mixed valence state [2^{2+}]⁺, K_c being comparable in magnitude to that of [**1**]⁺ and related terminal alkynyls.^{19e,28}

In the case of **3**, two irreversible oxidations are observed, the initial event showing a slight anodic shift relative to **1**, and indeed related alkynyl systems;^{19e,28} the second occurs at lower potential than the corresponding oxidation of [**1**]⁺. On the reverse scan, an irreversible reduction process is observed at heavily cathodic potential. Notably, the diminished separation of the oxidative events indicates a reduced stability for the mixed valence state ([**3**]⁺) in comparison to [**1**]⁺ and, indeed, related alkynyl complexes and [2^{2+}]⁺, K_c being two-orders of magnitude lower than for its counterparts.^{19e,28} Notwithstanding, some stability is apparent, which implies some retention of the electronic coupling characteristic of the “Ru₂{ μ -(C≡C)₂C₆H₄-p}” scaffold, albeit diminished by the seemingly electron-acceptor character of the cyaphide ligand.

Conclusions

In conclusion, we have described the first isolable compound to incorporate two ‘C≡P’ moieties as part of the same conju-



gated scaffold, viz. $[\text{Ru}_2\{\mu\text{-(C}\equiv\text{C)}_2\text{C}_6\text{H}_4\text{-p}\}\{\text{C}\equiv\text{P}\}_2]$ (**3**). The electronic spectrum shows a dominance of LLCT and MLCT transitions from the bridge and phosphacarbon moieties to the dppe scaffold, with negligible ILCT within the π -system. The redox properties of **3** are more interesting and suggest some electron-acceptor character for the cyaphide ligand. While its presence leads to irreversible redox behaviour and serves to destabilize the mixed-valent state $[\text{3}]^+$, the retention of electronic coupling within the bimetallic core provides initial conceptual validation for the incorporation of the cyaphide ligand into electro-active complexes. This will require engineering of appropriately stabilizing ancillary scaffolds, a challenge with which we are currently engaged.

Conflicts of interest

There are no conflicts to declare.

Acknowledgements

This work was supported by the Royal Society, Engineering and Physical Sciences Research Council (EPSRC; EP/N016785/1) and the University of Sussex (studentship to M. C. L.). I. R. C. gratefully acknowledges the award of a Royal Society University Research Fellowship. We thank Dr S. M. Roe (Sussex) for assistance with structural refinement for 2^{2+} .

Notes and references

- For reviews of phosphacarbon and phosphalkene chemistry see: (a) F. Mathey, *Angew. Chem., Int. Ed.*, 2003, **42**, 1578–1604; (b) R. Appel, in *Multiple Bonds and Low Coordination in Phosphorus Chemistry*, ed. M. Regitz and O. J. Scherer, Thieme, Stuttgart, 1990; (c) L. N. Markovski and V. D. Romanenko, *Tetrahedron*, 1989, **45**, 6019–6090; (d) R. Appel, F. Knoll and I. Ruppert, *Angew. Chem., Int. Ed. Engl.*, 1981, **20**, 731–744.
- K. B. Dillon, F. Mathey and J. F. Nixon, *Phosphorus: The Carbon Copy*, Wiley, Chichester, 1998.
- (a) J. F. Nixon, *Coord. Chem. Rev.*, 1995, **145**, 201–258; (b) J. F. Nixon, *Chem. Rev.*, 1988, **88**, 1327–1362.
- See for example and reviews: (a) C. Schubert, J. T. Margrat, T. Clark and D. M. Guidi, *Chem. Soc. Rev.*, 2015, **44**, 988–998; (b) P. J. Low, *Dalton Trans.*, 2005, 2821–2824; (c) M. I. Bruce and P. J. Low, *Adv. Organomet. Chem.*, 2004, **51**, 179–444; (d) M. I. Bruce and P. J. Low, *Adv. Organomet. Chem.*, 2001, **48**, 71–288; (e) F. Paul and C. Lapinte, *Coord. Chem. Rev.*, 1998, **178–180**, 431–509; (f) I. R. Whittall, A. J. McDonagh and M. G. Humphrey, *Adv. Organomet. Chem.*, 1998, **42**, 291–362; (g) N. J. Long, *Angew. Chem., Int. Ed. Engl.*, 1995, **34**, 21–38.
- (a) M. A. Shameem and A. Orthaber, *Chem. – Eur. J.*, 2016, **22**, 10718–10735; (b) T. Baumgartner, *Acc. Chem. Res.*, 2014, **47**, 1613–1622; (c) T. Baumgartner and R. Reau, *Chem. Rev.*, 2006, **106**, 4681–4727 and references therein.
- (a) X.-L. Geng, Q. Hu, B. Schafer and S. Ott, *Org. Lett.*, 2010, **12**, 692–695; (b) E. Oberg, B. Schafer, X.-L. Geng, J. Pettersson, Q. Hu, M. Kritikos, T. Rasmussen and S. Ott, *J. Org. Chem.*, 2009, **74**, 9265–9273; (c) B. Schafer, E. Oberg, M. Kritikoz and S. Ott, *Angew. Chem., Int. Ed.*, 2008, **47**, 8228–8231; (d) V. A. Wright, B. O. Patrick, C. Schneider and D. P. Gates, *J. Am. Chem. Soc.*, 2006, **126**, 8836–8844; (e) C.-W. Tsang, B. Baharloo, D. Riendi, M. Yam and D. P. Gates, *Angew. Chem., Int. Ed.*, 2004, **43**, 5682–5685; (f) C.-W. Tsang, M. Yam and D. P. Gates, *J. Am. Chem. Soc.*, 2003, **125**, 1480–1481.
- (a) X. He, J. Borau-Garcia, A. Y. Y. Woo, S. Trudel and T. Baumgartner, *J. Am. Chem. Soc.*, 2013, **135**, 1137–1147; (b) Y. Ren and T. Baumgartner, *Dalton Trans.*, 2012, **41**, 7792–7800; (c) P.-A. Bouit, A. Escande, R. Szucs, D. Szieberth, C. Lescop, L. Nyulaszi, M. Hissler and R. Reau, *J. Am. Chem. Soc.*, 2012, **134**, 6524–6527; (d) A. Bruch, A. Fukazawa, E. Yamaguchi, S. Yamaguchi and A. Studer, *Angew. Chem., Int. Ed.*, 2011, **50**, 12094–12098.
- (a) C. Mueller, R. Bartsch, A. Fischer, P. G. Jones and R. Schmutzler, *J. Organomet. Chem.*, 1996, **512**, 141–148; (b) R. Appel, G. Maier, H. P. Reisenauer and A. Westerhaus, *Angew. Chem., Int. Ed. Engl.*, 1981, **20**, 197–197.
- (a) C. Jones and M. Waugh, *J. Organomet. Chem.*, 2007, **692**, 5086–5090; (b) K. Toyota, S. Kawasaki and M. Yoshifuji, *J. Org. Chem.*, 2004, **69**, 5065–5070.
- (a) A. S. Ionkin, W. J. Marshall, B. M. Fish, A. A. Marchione, L. A. Howe, F. Davidson and C. N. McEwen, *Eur. J. Inorg. Chem.*, 2008, 2386–2390; (b) G. Markl and H. Sejpka, *Tetrahedron Lett.*, 1986, **27**, 171–174.
- M. Yoshifuji, H. Kawanami, Y. Kawai, K. Toyota, M. Yasunami, T. Niitsu and N. Inamoto, *Chem. Lett.*, 1992, **21**, 1053–1056.
- (a) T. A. Cooper, H. W. Kroto, J. F. Nixon and O. Ohashi, *J. Chem. Soc., Chem. Commun.*, 1980, 333–334; (b) H. W. Kroto, J. F. Nixon and K. Ohno, *J. Mol. Spectrosc.*, 1981, **90**, 512–516; (c) M. Brönstrup, J. Gottfriedsen, I. Kretzchmar, S. J. Blanksby, H. Schwarz and H. Schumann, *Phys. Chem. Chem. Phys.*, 2000, **2**, 2245–2250; (d) L. A. Jones, E. P. F. Lee, P. Soldan and T. G. Wright, *Phys. Chem. Chem. Phys.*, 1999, **1**, 391–395; (e) F. M. Bickelhaupt and F. Bickelhaupt, *Chem. – Eur. J.*, 1999, **5**, 162–174.
- (a) F. Brodkorb, M. Brym, C. Jones and C. Schulten, *J. Organomet. Chem.*, 2006, **691**, 1025–1029; (b) M. Brym and C. Jones, *Dalton Trans.*, 2003, 3665–3667.
- P. B. Hitchcock, M. J. Maah, J. F. Nixon, J. A. Zora, G. J. Leigh and M. A. Bakar, *Angew. Chem., Int. Ed. Engl.*, 1987, **26**, 474–475.
- S. M. Mansell, M. Green and C. A. Russell, *Dalton Trans.*, 2012, **41**, 14360–14368.
- N. Trathen, M. C. Leech, I. R. Crossley, V. K. Greenacre and S. M. Roe, *Dalton Trans.*, 2014, **43**, 9004–9007.



- 17 CCDC 1811689† Crystals grown from CH₂Cl₂/hexane at –20 °C. See ESI† for data.
- 18 (a) M. C. B. Colber, J. Lewis, N. J. Long, P. R. Raithby, A. J. P. White and D. J. Williams, *Dalton Trans.*, 1997, 99–104; (b) N. D. Jones and M. O. Wolf, *Organometallics*, 1997, **16**, 1352–1354; (c) C.-Y. Wong, C.-M. Che, M. C. W. Chan, J. Han, K.-H. Leung, D. L. Phillips, K.-Y. Wong and N. Zhu, *J. Am. Chem. Soc.*, 2005, **127**, 13997–14007; (d) A. Vacher, F. Barriere, T. Roisnel, L. Piekara-Sady and D. Lorcy, *Organometallics*, 2011, **30**, 3570–3578.
- 19 (a) S. Sporler, L. Muller, A. R. Waterloo, R. R. Tykwinski and N. Burzlaff, *J. Organomet. Chem.*, 2016, **821**, 122–129; (b) X. Wang, X. You, Z.-P. Shang and J. Xia, *J. Organomet. Chem.*, 2016, **803**, 111–118; (c) J. Xia, Y.-P. Ou, D. Wu, G. J. Jin, J. Yin, G.-A. Yu and S. H. Liu, *Dalton Trans.*, 2013, **42**, 14212–14222; (d) M. A. Fox, B. Le Guennic, R. L. Roberts, D. A. Brue, D. S. Yufit, J. A. K. Howard, G. Manca, J.-F. Halet, F. Hartl and P. J. Low, *J. Am. Chem. Soc.*, 2011, **133**, 18433–18446; (e) L. D. Field, A. M. Magill, T. K. Shearer, S. B. Colbran, S. T. Lee, S. J. Dalgarno and M. M. Bhadbhade, *Organometallics*, 2010, **29**, 957–965; (f) D. J. Armit, M. I. Bruce, M. Gaudio, N. N. Zaitseva, B. W. Skelton, A. H. White, B. L. Guennic, J.-F. Halet, M. A. Fox, R. L. Roberts, F. Hartl and P. J. Low, *Dalton Trans.*, 2008, 6763–6775.
- 20 (a) J. G. Cordaro, D. Stein, H. Ruegger and H. Grutzmacher, *Angew. Chem., Int. Ed.*, 2006, **45**, 6159–6162; (b) T. Groer, G. Baum and M. Scheer, *Organometallics*, 1998, **17**, 5916–5919.
- 21 Sub-stoichiometric KO^tBu affords statistical mixture of 2²⁺ and 3, with no evidence for the asymmetric (mono-desilylated) product. While separation of the mixture has not been effected, computed NMR data indicate signatures for the asymmetric species to be distinct from those of 2²⁺ and 3.
- 22 Geometries were optimized from an initial model based on the solid state structure of 2²⁺, using the B3LYP functional (lanl2dz for ruthenium; 6-31G** for all other atoms). See ESI† for full details.
- 23 C. Jones, C. Schulten and A. Stasch, *Eur. J. Inorg. Chem.*, 2008, 1555–1558.
- 24 J. C. T. R. Burckett-St. Laurent, M. A. King, H. W. Kroto, J. F. Nixon and R. J. Suffolk, *J. Chem. Soc., Dalton Trans.*, 1983, 755–759.
- 25 TD-DFT calculations were performed at the B3LYP level using lanl2dz for Ru and 3-21G* for all other atoms, without addition of a solvent model. Though a relatively low level of theory (constituting a balance against the complexity of the system and number of required excited states), such has previously proven suitable to provide a general guide to assignment.
- 26 Though commonly attributed to sequential Ru^{II}/Ru^{III} couples, the oxidation events have heavy involvement from the carbon-rich bridge, due to extensive orbital mixing in the HOMO. These are thus more properly considered as sequential mono-oxidations of the bimetallic core.
- 27 Though mindful of previous reports of 1 (and related systems) that describe the irreversible oxidation of [1]²⁺ close to 1 V,^{28b-e} in the present case we are confident in our assignment of this feature to oxidation of the mixed-valence complex [2²⁺]⁺ to [2²⁺]²⁺, the initial event being more consistent with a 1-electron process.
- 28 (a) E. Wuttke, Y.-M. Hervault, W. Polit, M. Linseis, P. Erler, S. Rigaut and R. F. Winter, *Organometallics*, 2014, **33**, 4672–4686; (b) A. Benameur, P. Brignou, E. D. Piazza, Y.-M. Hervault, L. Norel and S. Rigaut, *New J. Chem.*, 2011, **35**, 2105–2113; (c) C. Olivier, B. Kim, D. Touchard and S. Rigaut, *Organometallics*, 2008, **27**, 509–518; (d) A. Klein, O. Lavastre and J. Fielder, *Organometallics*, 2006, **25**, 635–643; (e) M. C. B. Colbert, J. Lewis, N. J. Long, P. R. Raithby, M. Younus, A. J. P. White, D. J. Williams, N. N. Payne, L. Yellowlees, D. Beljonne, N. Chawdhury and R. H. Friend, *Organometallics*, 1998, **17**, 3034–3043; (f) S. K. Hurst, M. P. Cifuentes, A. M. McDonagh, M. G. Humphrey, M. Samoc, B. Luther-Davies, I. Asselberghs and A. Persoons, *J. Organomet. Chem.*, 2002, **642**, 250–267; (g) O. Lavastre, J. Plass, P. Bachmann, S. Guesmi, C. Moinet and P. H. Dixneuf, *Organometallics*, 1997, **16**, 184–189.

